

International Journal of Modern Physics A  
© World Scientific Publishing Company

**CASIMIR EFFECT AS A TEST FOR THERMAL CORRECTIONS  
AND HYPOTHETICAL LONG-RANGE INTERACTIONS\***

G. L. KLIMCHITSKAYA

*North-West Technical University,  
Millionnaya St. 5, St.Petersburg, 191065, Russia  
Galina.Klimchitskaya@itp.uni-leipzig.de*

R. S. DECCA

*Department of Physics, Indiana University-Purdue University Indianapolis,  
Indianapolis, Indiana 46202, USA*

E. FISCHBACH

*Department of Physics, Purdue University,  
West Lafayette, Indiana 47907, USA*

D. E. KRAUSE

*Physics Department, Wabash College, Crawfordsville,  
Indiana 47933, USA*

D. LÓPEZ

*Bell Laboratories, Lucent Technologies,  
Murray Hill, New Jersey 07974, USA*

V. M. MOSTEPANENKO

*Noncommercial Partnership "Scientific Instruments",  
Tverskaya St. 11, Moscow, 103905, Russia*

*and*

*A. Friedmann Laboratory, St.Petersburg, Russia*

Received 16 November 2004

We have performed a precise experimental determination of the Casimir pressure between two gold-coated parallel plates by means of a micromachined oscillator. In contrast to all previous experiments on the Casimir effect, where a small relative error (varying from 1% to 15%) was achieved only at the shortest separation, our smallest experimental error ( $\sim 0.5\%$ ) is achieved over a wide separation range from 170 nm to 300 nm at 95% confidence. We have formulated a rigorous metrological procedure for the comparison of experiment and theory without resorting to the previously used root-mean-square deviation, which

\*This paper is the combined presentation of two talks given by G. L. Klimchitskaya and by V. M. Mostepanenko.

2 *G. L. Klimchitskaya et al.*

has been criticized in the literature. This enables us to discriminate among different competing theories of the thermal Casimir force, and to resolve a thermodynamic puzzle arising from the application of Lifshitz theory to real metals. Our results lead to a more rigorous approach for obtaining constraints on hypothetical long-range interactions predicted by extra-dimensional physics and other extensions of the Standard Model. In particular, the constraints on non-Newtonian gravity are strengthened by up to a factor of 20 in a wide interaction range at 95% confidence.

*Keywords:* Casimir force; Lifshitz theory; non-Newtonian gravity.

## 1. Introduction

The Casimir force<sup>1</sup> is a macroscopic quantum phenomenon arising from the modification of the zero-point oscillations of the electromagnetic field by material boundaries. It is in fact the limiting case of the well known van der Waals force when the separation distances between the test bodies are large enough for the manifestation of retardation effects. The modern experimental study of the Casimir force began in 1997 with Ref. 2 followed by Refs. 3–14. This work was stimulated both by the demands of nanotechnology, where the Casimir force may be large enough to drive nanoscale devices,<sup>10</sup> and also by the theory of fundamental interactions, where the Casimir effect plays a large role in testing the predictions of extra-dimensional physics.<sup>14</sup> Simultaneously with these new experiments, extensive theoretical work was carried out to refine calculations of the Casimir force by taking into account numerous correction factors such as finite conductivity of the boundary metal, nonzero temperature, surface roughness, and patch potentials among others (see Ref. 15 for a review).

Beginning in 2000, the behavior of the thermal correction to the Casimir force between real metals has been hotly debated. It was shown that Lifshitz theory,<sup>16</sup> which provides the theoretical foundation for the calculations of both the van der Waals and Casimir forces, leads to different results depending on the model of metal conductivity used. For real metals at low frequencies  $\omega$ , the dielectric permittivity  $\varepsilon$  varies as  $\omega^{-1}$ . After substituting  $\varepsilon \sim \omega^{-1}$  into the Lifshitz formula, the result is a thermal correction which is several hundred times greater than for ideal metals at separations of a few tenths of a micrometer.<sup>17,18</sup> The attempt<sup>19</sup> to modify the zero-frequency term of the Lifshitz formula for real metals, assuming that it behaves as in the case of ideal metals, also leads to a large thermal correction to the Casimir force at short separations.

It is important to note that in the approaches of both Refs. 17, 18 and also of Ref. 19 a thermodynamic puzzle arises, i.e., the Nernst heat theorem is violated for a perfect lattice.<sup>20,21</sup> (See also Ref. 22 where it is shown that for the preservation of the Nernst heat theorem in the approach of Refs. 17, 18 it is necessary to have metals with defects or impurities; it is common knowledge, however, that thermodynamics must be valid for both perfect and imperfect lattices.) This puzzle casts doubt on the many applications of the Lifshitz theory of dispersion forces, and thus represents a potentially serious challenge to both experimental and theoretical physics. By

contrast, the use of  $\varepsilon \sim \omega^{-2}$ , as holds in a free electron plasma model neglecting relaxation, leads<sup>23,24</sup> to a small thermal correction to the Casimir force at short separations. This is in qualitative agreement with the case of an ideal metal and is consistent with the Nernst heat theorem. It should be borne in mind, however, that the plasma model is not universal, and is applicable only in the case when the characteristic frequency is in the domain of infrared optics.

A universal theoretical approach consistent with thermodynamics was proposed in Ref. 25. It uses the Lifshitz formula with reflection coefficients expressed in terms of the surface impedance instead of the dielectric permittivity. In the framework of this approach one need not consider the zero-point and thermal photons inside a metal. The impedance approach was found to be consistent with the experimental results of Ref. 13, 14, whereas the alternative approaches of Refs. 17, 18 and Ref. 19 were excluded by this experiment. It should be noted, however, that in Refs. 13, 14 the contribution of surface roughness was rather large, and theory was compared with experiment by the use of the root-mean-square deviation (a method previously used in experiments on the Casimir force and criticized in literature<sup>9</sup>).

In the present paper we carry out a precise experimental determination of the Casimir pressure between two gold-coated parallel plates by means of a micro-machined oscillator. In contrast to all previous experiments on the Casimir force, the smallest experimental relative error (in our case from 0.55% to 0.6% at 95% confidence) was achieved not only at the shortest separations but rather in a wide separation range from 170 nm to 300 nm. The theoretical values of the Casimir pressure were calculated in the framework of each of the aforementioned approaches, taking careful account of all relevant corrections. The error in the theoretical results was found independently of the experimental errors. The distinguishing feature of our present comparison of experiment with theory is that we do not use the root-mean-square deviation. Instead, a rigorous metrological procedure is applied, which permits us to conclusively exclude the alternative approaches of Refs. 17–19 to the thermal Casimir force, and to thus resolve the puzzle arising from the violation of the Nernst heat theorem in these approaches. Our results are used to strengthen constraints on non-Newtonian gravity in the micrometer range by a factor of up to 20, and to significantly increase their reliability.

## 2. Setup, Measurement Procedure and Experimental Errors

The details of the experimental setup containing the micromachined oscillator (see Fig. 1) have already been presented in Refs. 13, 14. The vertical separation  $z$  between the sapphire sphere of radius  $R = (148.7 \pm 0.2) \mu\text{m}$  and a  $500 \times 500 \mu\text{m}^2$  heavily doped polysilicon plate (both coated with gold) was varied harmonically in time at the natural resonant frequency of the micromachined oscillator  $\omega_o = 2\pi \times 702.92 \text{ Hz}$ . Under the influence of the Casimir force  $F(z)$  acting between a plate and a sphere, the resonant frequency shifts, and from the measurement of this shift one can calculate  $\partial F(z)/\partial z$  (see Refs. 10, 13). Using the proximity force theorem,<sup>15</sup> we can

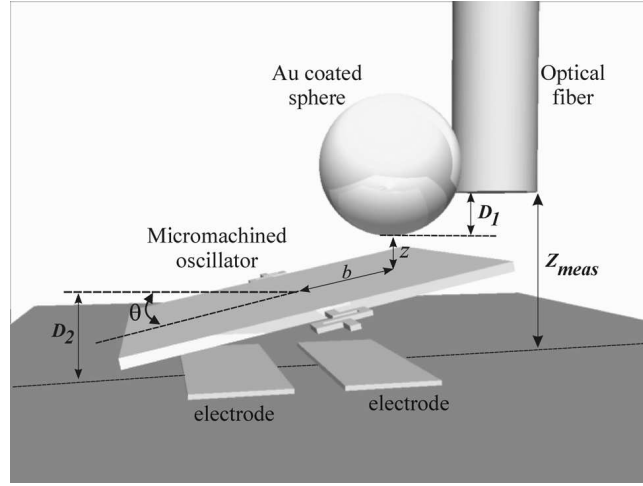


Fig. 1. Schematic of the experimental setup.

then find the equivalent Casimir pressure

$$P(z) = -\frac{1}{2\pi R} \frac{\partial F(z)}{\partial z} \quad (1)$$

between the two parallel plates, i.e., the Casimir force per unit area.

In the present experiment the setup was significantly improved in several ways, which permitted us to obtain results which considerably exceed those of Refs. 13, 14 in consistency and conclusiveness. First, the surface roughness was decreased by an order of magnitude on the sphere, and by a factor of five on the plate. This resulted in maximal heights of the roughness peaks equal to 11.06 nm and 20.63 nm, respectively. For the roughness characterization, the samples were studied with an AFM both before and after the Casimir force measurements. Second, the error in the measurements of the absolute separation  $z$  between the sphere and the plate was decreased from  $\Delta z = 1$  nm to  $\Delta z = 0.6$  nm at 95% confidence. The absolute separations were determined from  $z = z_{meas} - D - b\theta$  (see Fig. 1), where  $D = D_1 + D_2$  and the lever arm  $b = (210 \pm 3) \mu\text{m}$ . The quantity  $z_{meas}$  is measured interferometrically, and  $\theta$  is determined from the difference in capacitance between the plate and the right and left underlying electrodes. The value of  $D = (9349.7 \pm 0.5)$  nm was found from 120 plots of the electrostatic force as functions of separation at  $z > 3 \mu\text{m}$  (where the Casimir force is negligible) for the given potential differences between a sphere and a plate. Third, shorter separation distances between the sphere and the plate were achieved (160 nm instead of 260 nm) owing to an improvement in detection sensitivity, and to a decrease of the coupling between the micromachined

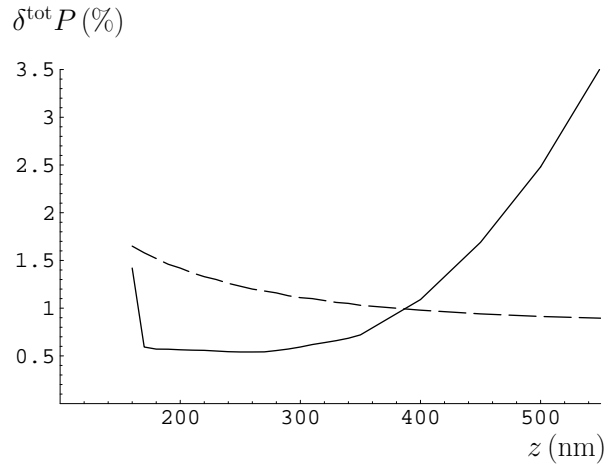


Fig. 2. The total relative errors of our experimental (solid line) and theoretical (dashed line) Casimir pressures versus separation.

oscillator and the environment. In doing so we verified that the response of the micromachined oscillator was still linear. Fourth, a gold coating was used on both test bodies (instead of the dissimilar metals as in Refs. 13, 14) which makes the theoretical interpretation of the final results more transparent. As a result, the Casimir pressure  $P^{\text{expt}}(z)$  was measured within a separation range from 160 nm to 750 nm. This measurement was repeated fifteen times with 288–293 points in each run. Each individual point was obtained with an integration time of 10 s.

The experimental data were analyzed for the presence of outlying results by the use of statistical criteria,<sup>26</sup> and one of the fifteen sets of measurements was found to be outlying. All data from the remaining fourteen sets were plotted as a function of separation for separation distances between 160 nm and 750 nm, where the total separation interval was divided into partial subintervals of length  $2\Delta z = 1.2$  nm each. The measurement data were carefully analyzed and found to be uniform in mean values, but not uniform in variance. Because of this, the random error as a function of separation was found using a special procedure developed from the theory of repeated measurements.<sup>27,28</sup>

The systematic errors in the Casimir pressure determination were found to arise from the error in sphere radius  $\Delta R = 0.2 \mu\text{m}$ , and from the error in the angular resonant frequency  $\Delta\omega_o = 2\pi \times 6 \text{ mHz}$ . To obtain the total experimental error of our measurements, it is necessary to combine the random and systematic errors which are described by the normal or Student and uniform distributions, respectively. Finally, the total relative experimental error as a function of separation was determined at 95% confidence (see solid line in Fig. 2). As is seen from Fig. 2, the smallest experimental error from 0.55% to 0.6% is achieved, not only at the shortest separation (as in all previous Casimir force measurements where the error was also

6 *G. L. Klimchitskaya et al.*

larger), but in a wide range from 170 nm to 300 nm. This opens new opportunities to use our results for imposing stronger constraints on thermal effects and on hypothetical long-range interactions.

### 3. Theory, Theoretical Errors and Comparison with Experiment

In addition to performing the measurements, we calculated the equivalent Casimir pressure acting between two gold-coated plates in thermal equilibrium at a temperature  $T = 300$  K using the Lifshitz formula<sup>16</sup>

$$P(z) = -\frac{k_B T}{\pi} \sum_{l=0}^{\infty} \int_0^{\infty} k_{\perp} dk_{\perp} q_l \times \left\{ \left[ r_{\parallel}^{-2}(\xi_l, k_{\perp}) e^{2q_l z} - 1 \right]^{-1} + \left[ r_{\perp}^{-2}(\xi_l, k_{\perp}) e^{2q_l z} - 1 \right]^{-1} \right\}. \quad (2)$$

Here  $q_l^2 = k_{\perp}^2 + \xi_l^2/c^2$  and the summation is performed with respect to the Matsubara frequencies  $\xi_l = 2\pi k_B T l/\hbar$ , where  $k_B$  is the Boltzmann constant,  $l = 0, 1, 2, \dots$ , and the prime adds a factor 1/2 for the  $l = 0$  term. The reflection coefficients  $r_{\parallel, \perp}$  also depend on the magnitude of a wave vector component in the plane of plates  $k_{\perp} = |\mathbf{k}_{\perp}|$ .

As was shown in Ref. 25, in order for the Lifshitz formula to avoid contradictions with thermodynamics for real metals, the reflection coefficients should be expressed in terms of the surface impedance  $Z(\omega)$ :

$$r_{\parallel}^{-2}(\xi_l, k_{\perp}) = \left[ \frac{Z(i\xi_l)\xi_l + cq_l}{Z(i\xi_l)\xi_l - cq_l} \right]^2, \quad r_{\perp}^{-2}(\xi_l, k_{\perp}) = \left[ \frac{Z(i\xi_l)cq_l + \xi_l}{Z(i\xi_l)cq_l - \xi_l} \right]^2. \quad (3)$$

The values of the impedance at all contributing imaginary Matsubara frequencies with  $l \geq 1$  are given by  $Z(i\xi_l) = 1/\sqrt{\varepsilon(i\xi_l)}$  (which is the so called Leontovich impedance<sup>29</sup>), where  $\varepsilon(i\xi_l)$  is calculated by means of a dispersion relation from the tabulated<sup>30</sup> complex refraction index of Au (see, e.g., Ref. 31 for the details of the calculation procedure). When the Matsubara frequency is zero, the value of the impedance should be obtained<sup>25</sup> by extrapolation from the region of characteristic frequencies, which is infrared optics in our case, resulting in  $Z(i\xi) \approx \xi/\omega_p$  when  $\xi \rightarrow 0$ , where  $\omega_p$  is the plasma frequency. From Eq. (3) one then arrives at

$$r_{\parallel}^{-2}(0, k_{\perp}) = 1, \quad r_{\perp}^{-2}(0, k_{\perp}) = \left( \frac{ck_{\perp} + \omega_p}{ck_{\perp} - \omega_p} \right)^2. \quad (4)$$

The use of the Leontovich impedance in Eq. (3) which does not depend on the polarization state and transverse momentum, is of prime importance. Note that in Refs. 32, 33 the exact impedances depending on a transverse momentum were used. This has led to the same conclusions as were obtained previously from the Lifshitz formula combined with the dielectric permittivity  $\varepsilon \sim \omega^{-1}$ . As was already mentioned above, these conclusions are in violation of the Nernst heat theorem for a perfect lattice.<sup>20–22</sup> Although a recent review<sup>33</sup> claims agreement with the

Nernst heat theorem in Refs. 17, 18, no specific objections against the rigorous analytical proof of the opposite statement in Ref. 21 are presented. The fallacy in the calculations of Refs. 32, 33 concerning the type of the impedance is that they disregard the requirement that the reflection properties for virtual photons on a classical boundary should be the same as for real photons. Ref. 21 demonstrates in detail that by enforcing this requirement the exact and Leontovich impedances coincide at zero frequency and lead to the conclusions of Ref. 25 which are in perfect agreement with the Nernst heat theorem.

In fact, the exact impedances, depending on both polarization state and transverse momentum are<sup>21,32,33</sup>

$$Z_{\parallel}(\omega, k_{\perp}) = \frac{1}{\sqrt{\varepsilon(\omega)}} \left[ 1 - \frac{c^2 k_{\perp}^2}{\varepsilon(\omega) \omega^2} \right]^{1/2}, \quad (5)$$

$$Z_{\perp}(\omega, k_{\perp}) = \frac{1}{\sqrt{\varepsilon(\omega)}} \left[ 1 - \frac{c^2 k_{\perp}^2}{\varepsilon(\omega) \omega^2} \right]^{-1/2}.$$

The angle of incidence  $\theta_0$  of a plane electromagnetic wave with a wave vector  $\mathbf{k}$  from vacuum on the boundary plane of a metal is evidently given by  $\sin \theta_0 = k_{\perp}/|\mathbf{k}|$ . The important requirement is that the reflection properties of virtual photons on a classical boundary are the same as of real ones. In particular, the angle of reflection must be equal to the angle of incidence, i.e., the first Snell's law must be satisfied. This law follows from the fact that for reflection at a classical boundary, the mass-shell equation  $|\mathbf{k}| = \omega/c$  is valid leading to  $\sin \theta_0 = ck_{\perp}/\omega$ . Substituting this into Eq. (5) and expanding in powers of a small parameter  $\sin^2 \theta_0/\varepsilon$ , we arrive at

$$Z_{\parallel}(\omega, k_{\perp}) = \frac{1}{\sqrt{\varepsilon(\omega)}} \left[ 1 - \frac{\sin^2 \theta_0}{\varepsilon(\omega)} \right]^{1/2} = Z(\omega) \left[ 1 - \frac{\sin^2 \theta_0}{2\varepsilon(\omega)} + \dots \right], \quad (6)$$

$$Z_{\perp}(\omega, k_{\perp}) = \frac{1}{\sqrt{\varepsilon(\omega)}} \left[ 1 - \frac{\sin^2 \theta_0}{\varepsilon(\omega)} \right]^{-1/2} = Z(\omega) \left[ 1 + \frac{\sin^2 \theta_0}{2\varepsilon(\omega)} - \dots \right],$$

where  $Z(\omega)$  is the Leontovich impedance.

In metals for all frequencies which are at least several times smaller than the plasma frequency  $|\varepsilon| \gg 1$  holds. For this reason, the term  $\sin^2 \theta_0/\varepsilon$  in Eq. (6) can be neglected in comparison with unity. An important point is that  $|\sin^2 \theta_0/\varepsilon| \rightarrow 0$  when  $\omega \rightarrow 0$ , i.e., at zero frequency the Leontovich impedance precisely coincides with the exact impedances. This is in contradiction with Refs. 32, 33, where the limit  $\omega \rightarrow 0$  was considered at fixed nonzero  $k_{\perp}$ . The latter violates the mass-shell equation and, consequently, necessitates postulating some unusual reflection properties for virtual photons on a classical boundary. As a result, the use of the Leontovich impedance, which is in fact exact at zero frequency, is in agreement with thermodynamics, whereas the approach of Refs. 32, 33 leads to the previous conclusions<sup>18</sup> which are in contradiction with fundamental physical principles.

The claims of Ref. 33 against the extrapolation of Eq. (4) to the zero Matsubara frequency also collapse.<sup>34</sup> As is shown in Ref. 34, the alternative extrapolation, suggested in Ref. 33, leads to the unsupportable violation of the Nernst heat theorem.

Using Eqs. (2)–(4), the Casimir pressures  $P(z)$  were computed within the measurement separation range. It can be seen<sup>8</sup> that small sample-to-sample variations of the tabulated data for the refractive index due to, for example, differences in the grain size distribution and the presence of impurities, lead to a decrease in the magnitude of the Casimir pressure which is much less than 0.5% even at the shortest separation  $z = 160$  nm considered here. Note also that at separations  $160 \text{ nm} \leq z \leq 750$  nm the effects of spatial dispersion do not lead to any noticeable contribution to the Casimir pressure.<sup>35</sup>

The other correction factors which may influence the values of the theoretical Casimir pressure are the surface roughness and patch potentials. The AFM study of both interacting surfaces shows that the characteristic lateral size of the surface distortions is approximately 500–600 nm, i.e., a factor of three larger than the shortest separations in our experiment. In this case the roughness correction can be found<sup>36</sup> by geometrical averaging,<sup>4,15</sup> which leads to the conclusion that the largest roughness correction achieved here at the shortest separation ( $z = 160$  nm) is only 0.65% of the Casimir pressure (and 0.42% at  $z = 200$  nm). It is easily seen that the contribution of diffraction-type and correlation effects to the roughness correction, which cannot be found by the additive method, is of order of 0.01%. The contributions of patch potentials, which are of the same order, and thus negligible, were found in analogy with Ref. 8. The values of the Casimir pressure  $P^{\text{theor}}(z)$  including roughness corrections were computed at all 4066 experimental points.

We are now in a position to determine the error in the theoretical results. The main sources of errors are the proximity force theorem [see Eq. (1)], which leads<sup>37–39</sup> to a relative error in the Casimir pressure less than  $z/R$ , and an uncertainty in the tabulated data for the complex refractive index leading to an error less than 0.5%. Both of these errors in the pressure are approximately described by a uniform distribution. One should also take into account that, for purposes of comparison with experiment, the theoretical pressure is computed at the experimental points defined with an error  $\Delta z$ . Since the Casimir pressure depends on the inverse fourth power of the separation, this leads<sup>40</sup> to a relative error  $4\Delta z/z$ . Combining the above three errors at 95% confidence, we obtain the theoretical relative error of the Casimir pressure calculations shown by the dashed line in Fig. 2. As is seen from Fig. 2, at separations  $z < 390$  nm the experimental error is less than the theoretical error.

With independently determined experimental and theoretical errors at our disposal, it becomes possible to find the total absolute error of the new random variable [ $P^{\text{theor}}(z) - P^{\text{expt}}(z)$ ] at 95% confidence. In this way we avoid the use of the root-mean-square deviation between theory and experiment which was applied in previous Casimir force measurements. In Ref. 9 this procedure was demonstrated

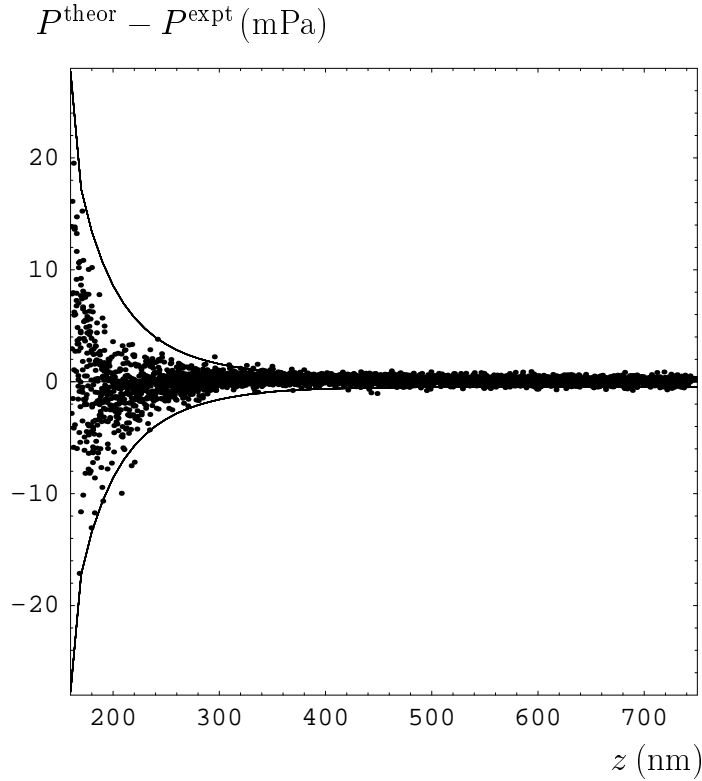


Fig. 3. Differences of our theoretical and experimental Casimir pressures (dots) and 95% confidence interval (solid lines) versus separation for all fourteen sets of measurements.

to be inadequate when the force increases rapidly with the decrease of separation, although no alternative approach was proposed. In Fig. 3 the confidence interval  $[-\Delta^{\text{tot}}(P^{\text{theor}} - P^{\text{expt}}), \Delta^{\text{tot}}(P^{\text{theor}} - P^{\text{expt}})]$  is shown by the solid lines as a function of separation. In the same figure the differences between our theoretical and experimental Casimir pressures are plotted by points for all fourteen sets of measurements. Remarkably, only 207 points (i.e., 5.09% of the total number) fall outside of the confidence interval, which demonstrates excellent agreement between our theory and experiment. The relative measure of agreement between theory and experiment is  $\Delta^{\text{tot}}(P^{\text{theor}} - P^{\text{expt}})/|P^{\text{theor}}|$ . This is equal to 1.9% at  $z = 170$  nm, 1.4% within the interval  $270 \text{ nm} \leq z \leq 370$  nm, 1.8% at  $z = 420$  nm, and then increases up to 13% at  $z = 750$  nm. Thus our experiment is the first measurement of the Casimir force where agreement between theory and experiment at the level of 1.5% has been achieved at high confidence within a wide separation region.

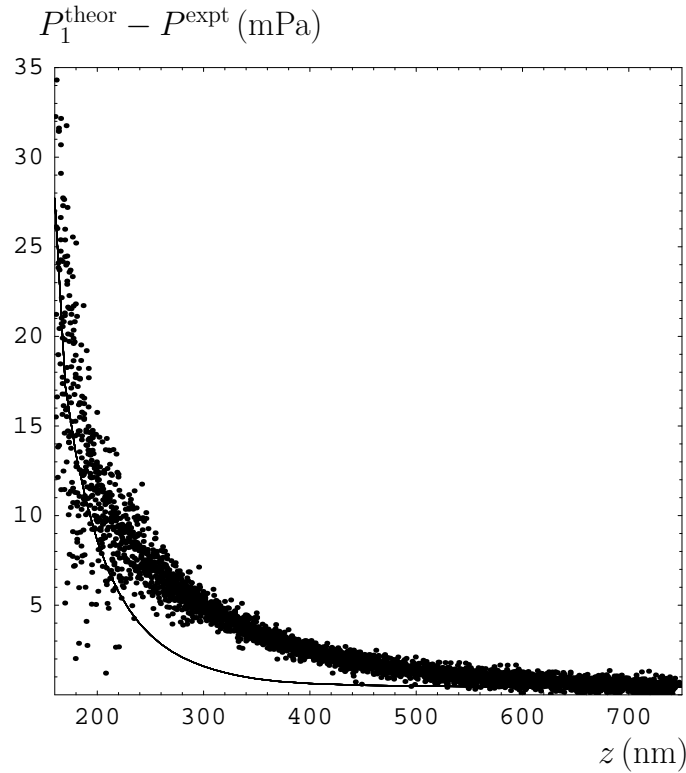


Fig. 4. Differences of theoretical<sup>17,18</sup> and experimental Casimir pressures (dots) and a positive half of a 95% confidence interval (solid line) versus separation for all fourteen sets of measurements.

#### 4. Alternative Theories and Resolution of a Thermodynamic Puzzle

This experiment, and the extent of agreement between our measurements and theory, can be used to test the alternative theoretical approaches to the thermal Casimir force proposed in Refs. 17–19, and to thus finally resolve the contradiction between these approaches and thermodynamics. Refs. 17–19 use the Lifshitz formula in Eq. (2) with the reflection coefficients expressed in terms of the dielectric permittivity

$$r_{\parallel,L}^{-2}(\xi_l, k_{\perp}) = \left[ \frac{k_l + \varepsilon(i\xi_l)q_l}{k_l - \varepsilon(i\xi_l)q_l} \right]^2, \quad r_{\perp,L}^{-2}(\xi_l, k_{\perp}) = \left[ \frac{k_l + q_l}{k_l - q_l} \right]^2, \quad (7)$$

where  $k_l^2 = k_{\perp}^2 + \varepsilon(i\xi_l)\xi_l^2/c^2$ . The values of  $\varepsilon(i\xi)$  in Refs. 17–19 were found in the same way as described above. In fact the use of the Lifshitz reflection coefficients (7) instead of the impedance coefficients (3) leads to only minor differences at all  $l \geq 1$ . The major difference in the approaches of Refs. 17–19 is the value of the zero-frequency term of the Lifshitz formula. In Refs. 17, 18 (see also Refs. 32, 33) the

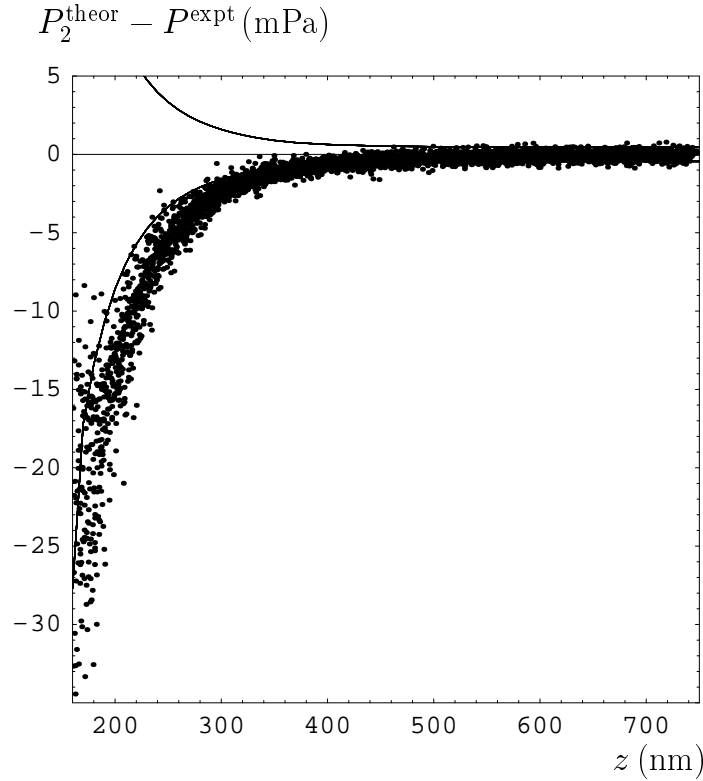


Fig. 5. Differences of theoretical<sup>19</sup> and experimental Casimir pressures (dots) and 95% confidence interval (solid lines) versus separation for all fourteen sets of measurements.

Drude dielectric function, depending on frequency as  $\varepsilon \sim \omega^{-1}$  when  $\omega \rightarrow 0$ , was substituted into Eq. (7) leading to  $r_{\parallel,L}^2(0, k_{\perp}) = 1$ ,  $r_{\perp,L}^2(0, k_{\perp}) = 0$  instead of Eq. (4). In Ref. 19 it was postulated that  $r_{\parallel}^2(0, k_{\perp}) = r_{\perp}^2(0, k_{\perp}) = 1$  as for ideal metals. In Figs. 4,5 we plot the differences of the Casimir pressures  $[P_{1,2}^{\text{theor}} - P^{\text{expt}}]$  versus separation computed in the approaches of Refs. 17, 18 and Ref. 19, respectively, with their respective confidence intervals at 95% confidence. As is seen from Fig. 4, all points representing  $[P_1^{\text{theor}} - P^{\text{expt}}]$  obtained according to Refs. 17, 18 fall outside the confidence interval in a wide separation range from 230 nm to 500 nm. (In Fig. 4 the symmetric negative line of the error bars is not shown because practically all points are positive.) From Fig. 5 it is seen that almost all points representing  $[P_2^{\text{theor}} - P^{\text{expt}}]$  obtained according to Ref. 19 fall outside the confidence interval for separations from 160 nm to 350 nm. Thus, the theoretical approaches of both Refs. 17, 18 and 19 are not only in contradiction with thermodynamics but also are excluded experimentally at 95% confidence.

12 *G. L. Klimchitskaya et al.*

It is easily seen that for the theory of Refs. 17, 18 the confidence interval can be widened to achieve 99% confidence probability. Even in this case almost all differences  $[P_1^{\text{theor}} - P^{\text{expt}}]$  fall outside the new confidence interval in the separation region  $300 \text{ nm} \leq z \leq 500 \text{ nm}$ . We conclude that the theoretical approach to the thermal Casimir force extensively discussed in Refs. 17, 18, 32, 33 is excluded experimentally with 99% confidence. This brings a final resolution to the thermodynamic puzzle arising from the thermal Casimir force.

## 5. Constraints on Hypothetical Long-Range Interactions

The probable existence of long-range interactions, in addition to gravitation and electromagnetism, has long been discussed in elementary particle physics.<sup>14</sup> They are predicted by extra-dimensional theories with low compactification scale,<sup>41</sup> and can also arise from the exchange of light or massless elementary particles predicted by many extensions to the Standard Model.<sup>15</sup> In many cases the effective potential energy between two point masses  $m_1$  and  $m_2$  at a distance  $r$  can be parametrized by the Newton gravitational potential with a Yukawa-type correction<sup>42</sup>

$$V(r) = -\frac{Gm_1m_2}{r} \left(1 + \alpha_G e^{-r/\lambda}\right), \quad (8)$$

where  $G$  is the gravitational constant,  $\alpha_G$  and  $\lambda$  are the strength and interaction range of the hypothetical force, respectively.

The constraints on corrections to Newtonian gravity follow from experiments of the Eötvos- and Cavendish-type. The most stringent constraints to date are presented in Fig. 6. In this figure, the regions of  $(\lambda, \alpha_G)$ -plane above the curves are excluded by the results of the indicated experiments, and the regions below the curves are allowed. Curves 1 and 2 show the constraints following from the Eötvos-type experiments of Refs. 43 and 44, respectively. Curves 3–6 follow from the Cavendish-type experiments of Refs. 45–48, respectively. Constraints on  $\alpha_G$  at astronomical scales of  $\lambda$  can be found in Ref. 42.

As is seen from Fig. 6, rather strong constraints on the corrections to Newtonian gravity are obtained within the interaction range  $\lambda > 0.1 \text{ m}$ . With decreasing  $\lambda$  the strength of constraints falls off rapidly. Curve 7 exhibits the constraints which follow<sup>49</sup> not from gravitational experiments but from a measurement of the Casimir force between a plate and a spherical lens by means of a torsion pendulum.<sup>2</sup> Many other constraints on corrections to Newtonian gravity in the submicrometer range were obtained from different Casimir force measurements (see Ref. 50 for a review).

As was already noted above, in all previous experiments on the Casimir effect the root-mean-square deviation  $\sigma$  was used as a measure of agreement between theory and experiment. No evidence for hypothetical long-range interactions has been observed in any experiments. For this reason the constraints on  $\alpha_G$ ,  $\lambda$  were usually obtained from the inequality

$$|F^{\text{hyp}}(z)| \leq \sigma. \quad (9)$$

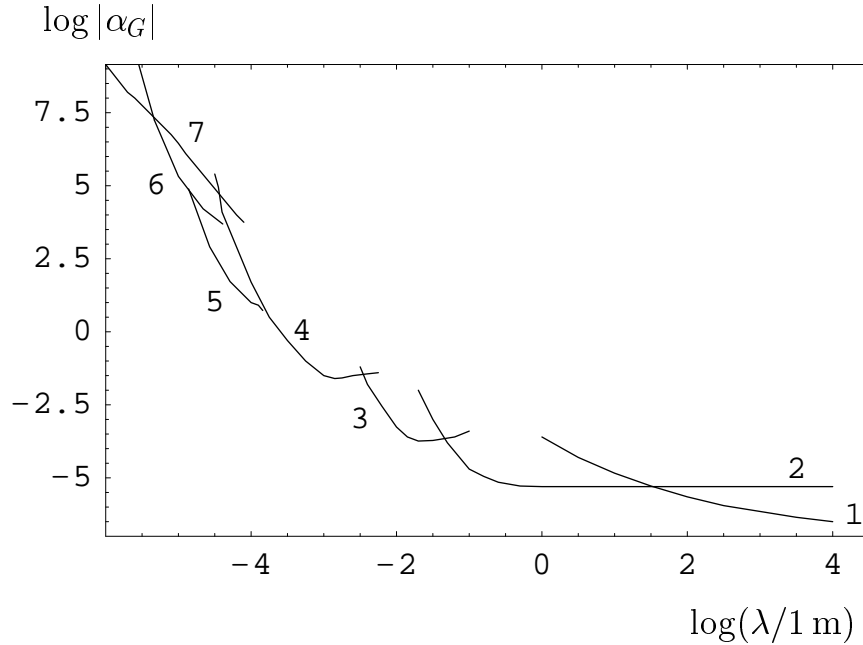


Fig. 6. Constraints on the strength of the Yukawa-type interaction  $\alpha_G$  versus interaction range  $\lambda$  obtained from the experiments of Eötvos-type (curves 1, 2), Cavendish-type (curves 3–6) and from the measurements of the Casimir force (curve 7). See text for a more detailed characterization of the curves.

In doing so it was not possible to quantify the reliability and the confidence level of the resulting constraints.

The new rigorous approach to the comparison of experiment and theory in the Casimir force measurements, developed here, gives the possibility of obtaining constraints on a hypothetical Yukawa-type pressure from the agreement of our measurements and theory at 95% confidence. We have found an agreement between our measurements of the Casimir pressure and theory in the limits of the error band  $\Delta^{\text{tot}}$  calculated at a confidence probability 95%. Because of this, the pressure of any hypothetical force must satisfy the inequality

$$|P^{\text{hyp}}(z)| \leq \Delta^{\text{tot}} [P^{\text{theor}}(z) - P^{\text{expt}}(z)]. \quad (10)$$

It should be stressed that the use of our data to decide among several competing theories of the thermal Casimir force by no means prevents us from using the same data to impose stronger constraints on hypothetical long-range interactions once the choice was made. The reason is that the Yukawa-type hypothetical pressure depends on separation quite differently from the alternative thermal corrections discussed above. Thus, the mimicry of one phenomenon by another one is not possible. We

14 *G. L. Klimchitskaya et al.*

also note that surface roughness, which was significantly reduced in this experiment, does not give any noticeable contribution to a hypothetical interaction of the Yukawa type with an interaction range of about 100 nm. Because of this, in calculations of the hypothetical force one can consider the test bodies to be perfectly smooth.

The equivalent hypothetical pressure in the configuration of two parallel plates (one made of Si and coated with Pt and Au layers, the other one made of  $\text{Al}_2\text{O}_3$  and coated with Ti and Au layers) is given by<sup>14</sup>

$$\begin{aligned}
 P^{\text{hyp}}(z) = & -2\pi G\alpha_G\lambda^2 e^{-z/\lambda} \\
 & \times \left[ \rho_{Au} - (\rho_{Au} - \rho_{Ti}) e^{-\Delta_{Au}^s/\lambda} - (\rho_{Ti} - \rho_{AlO}) e^{-(\Delta_{Au}^s + \Delta_{Ti})/\lambda} \right] \\
 & \times \left[ \rho_{Au} - (\rho_{Au} - \rho_{Pt}) e^{-\Delta_{Au}^p/\lambda} - (\rho_{Pt} - \rho_{Si}) e^{-(\Delta_{Au}^p + \Delta_{Pt})/\lambda} \right].
 \end{aligned} \quad (11)$$

Here the mass densities are given by  $\rho_{AlO} = 4.1 \times 10^3 \text{ kg/m}^3$ ,  $\rho_{Ti} = 4.51 \times 10^3 \text{ kg/m}^3$ ,  $\rho_{Au} = 19.28 \times 10^3 \text{ kg/m}^3$ ,  $\rho_{Si} = 2.33 \times 10^3 \text{ kg/m}^3$ ,  $\rho_{Pt} = 21.47 \times 10^3 \text{ kg/m}^3$ , and the thicknesses of layers are  $\Delta_{Ti} = 10 \text{ nm}$ ,  $\Delta_{Au}^s = 200 \text{ nm}$ ,  $\Delta_{Pt} = 10 \text{ nm}$ ,  $\Delta_{Au}^p = 150 \text{ nm}$ . Eq. (11) was derived under the conditions  $z, \lambda \ll R, L$ , where  $L = 3.5 \mu\text{m}$  is the

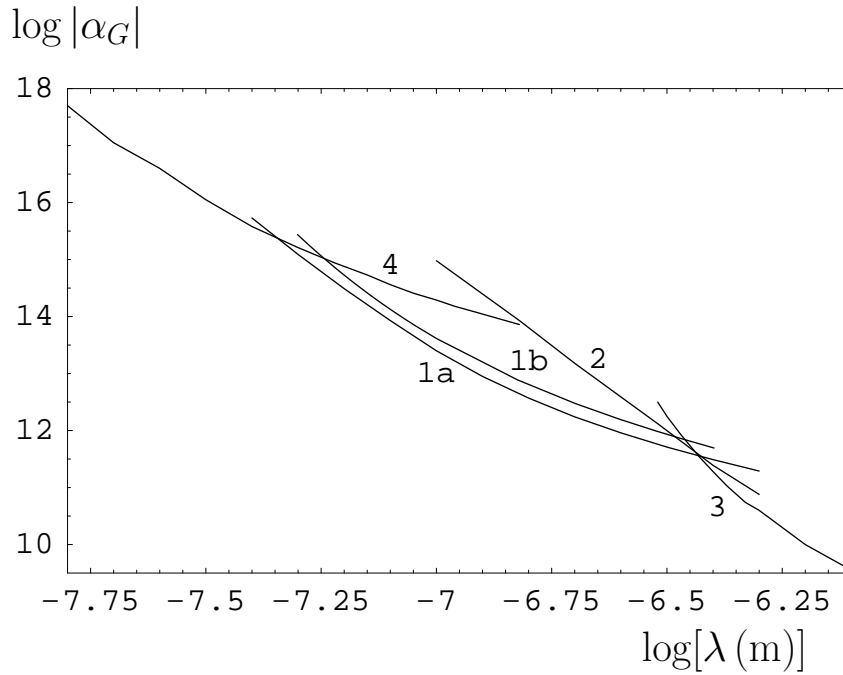


Fig. 7. Constraints on the strength of the Yukawa-type interaction  $\alpha_G$  versus interaction range  $\lambda$  obtained from the Casimir force measurements of the present paper (curve 1a) and earlier measurements of the Casimir force (curves 1b, 2-4). See text for a more detailed characterization of the curves.

thickness of the Si plate.

Constraints obtained from Eq. (10) after the substitution of Eq. (11) are plotted by curve 1a in Fig. 7. At each  $\lambda$  the separation  $z$  was found leading to the strongest constraint. (As a rule, the greater  $\lambda$ , the greater is  $z$  where the strongest constraint is obtained.) In the same figure curve 1b shows constraints obtained from the previous experiment of Ref. 14, curve 2 — from an old Casimir force measurement between dielectrics,<sup>15</sup> curve 3 — from the Casimir force measurement of Ref. 2 (this curve was labeled 7 in Fig. 6). Curve 4 was obtained<sup>51</sup> from an experiment measuring the Casimir force by the use of an atomic force microscope.<sup>7</sup> Note that the constraints of curve 1a obtained here are not only the most stringent ones in the interaction range  $40 \text{ nm} \leq \lambda \leq 370 \text{ nm}$ , but they are also valid at a 95% confidence, i.e., with a greater reliability than the other constraints in Fig. 7 for which the confidence levels were not determined. The largest improvement, comparing curves 2 and 4 with 1a, is by a factor of 20, and is achieved at  $\lambda \approx 150 \text{ nm}$ .

## 6. Conclusions and Discussion

To conclude, we have first experimentally determined the Casimir pressure between two parallel gold-coated plates with a relative error of approximately 0.5% at 95% confidence within a wide separation range. The surface impedance approach to the thermal Casimir force, and two alternative theoretical approaches advocated in literature, were compared with experiment in a statistically valid way without recourse to the root-mean-square deviation. This permitted us to experimentally exclude the alternative theoretical approaches which predict large thermal corrections at short separations, and to thus resolve the thermodynamic puzzle extensively discussed during the past few years. The thermal correction predicted by the impedance approach to the thermal Casimir force was found to be consistent with experiment. At  $T = 300 \text{ K}$  this correction is small, in qualitative agreement with the case of ideal metals, and can be readily measured by means of proposed experiments.<sup>52,53</sup>

Our results lay the groundwork for more precise calculations of the Casimir forces between closely spaced surfaces, thin films, and small particles near a cavity wall for applications in nanotechnology, quantum optics, biology and colloid science. These results significantly enhance constraints on predictions of extra-dimensional physics and other extensions to the Standard Model. Specifically, constraints on the Yukawa-type hypothetical interaction were strengthened by a factor of up to 20 within a wide interaction range at 95% confidence probability.

### *Acknowledgments*

The authors thank H. B. Chan for technical assistance in sample preparation. G. L. Klimchitskaya and V. M. Mostepanenko are grateful to T. N. Siraya for several helpful discussions on the metrological procedures of data analysis. They acknowledge financial support and kind hospitality from Purdue University. The work of R. S. Decca and E. Fischbach was supported in part by the Petroleum Research

16 *G. L. Klimchitskaya et al.*

Foundation (through ACS-PRF No.37542-G) and the U.S. Department of Energy (under Contract No. DE-AC02-76ER071428), respectively.

## References

1. H. B. G. Casimir, *Proc. K. Ned. Akad. Wet.* **51**, 793 (1948).
2. S. K. Lamoreaux, *Phys. Rev. Lett.* **78**, 5 (1997).
3. U. Mohideen and A. Roy, *Phys. Rev. Lett.* **81**, 4549 (1998).
4. G. L. Klimchitskaya, A. Roy, U. Mohideen and V. M. Mostepanenko, *Phys. Rev.* **A60**, 3487 (1999).
5. A. Roy and U. Mohideen, *Phys. Rev. Lett.* **82**, 4380 (1999).
6. A. Roy, C.-Y. Lin and U. Mohideen, *Phys. Rev.* **D60**, 111101(R) (1999).
7. B. W. Harris, F. Chen and U. Mohideen, *Phys. Rev.* **A62**, 052109 (2000).
8. F. Chen, G. L. Klimchitskaya, U. Mohideen and V. M. Mostepanenko, *Phys. Rev.* **A69**, 022117 (2004).
9. T. Ederth, *Phys. Rev.* **A62**, 062104 (2000).
10. H. B. Chan, V. A. Aksyuk, R. N. Kleiman, D. J. Bishop and F. Capasso, *Science* **291**, 1941 (2001); *Phys. Rev. Lett.* **87**, 211801 (2001).
11. G. Bressi, G. Carugno, R. Onofrio and G. Ruoso, *Phys. Rev. Lett.* **88**, 041804 (2002).
12. F. Chen, U. Mohideen, G. L. Klimchitskaya and V. M. Mostepanenko, *Phys. Rev. Lett.* **88**, 101801 (2002); *Phys. Rev.* **A66**, 032113 (2002).
13. R. S. Decca, D. López, E. Fischbach and D. E. Krause, *Phys. Rev. Lett.* **91**, 050402 (2003).
14. R. S. Decca, E. Fischbach, G. L. Klimchitskaya, D. E. Krause, D. López and V. M. Mostepanenko, *Phys. Rev.* **D68**, 116003 (2003).
15. M. Bordag, U. Mohideen and V. M. Mostepanenko, *Phys. Rep.* **353**, 1 (2001).
16. E. M. Lifshitz, *Zh. Eksp. Teor. Fiz.* **29**, 94 (1956) [*Sov. Phys. JETP* **2**, 73 (1956)]; I. E. Dzyaloshinskii, E. M. Lifshitz and L. P. Pitaevskii, *Usp. Fiz. Nauk* **73**, 381 (1961) [*Sov. Phys. Usp.* **4**, 153 (1961)].
17. M. Boström and B. E. Sernelius, *Phys. Rev. Lett.* **84**, 4757 (2000).
18. J. S. Høye, I. Brevik, J. B. Aarseth and K. A. Milton, *Phys. Rev.* **E67**, 056116 (2003).
19. V. B. Svetovoy and M. V. Lokhanin, *Mod. Phys. Lett.* **A15**, 1013 (2000); **A15**, 1437 (2000).
20. V. B. Bezerra, G. L. Klimchitskaya and V. M. Mostepanenko, *Phys. Rev.* **A66**, 062112 (2002).
21. V. B. Bezerra, G. L. Klimchitskaya, V. M. Mostepanenko and C. Romero, *Phys. Rev.* **A69**, 022119 (2004).
22. M. Boström and B. E. Sernelius, *Physica* **A339**, 53 (2004).
23. C. Genet, A. Lambrecht and S. Reynaud, *Phys. Rev.* **A62**, 012110 (2000).
24. M. Bordag, B. Geyer, G. L. Klimchitskaya and V. M. Mostepanenko, *Phys. Rev. Lett.* **85**, 503 (2000).
25. B. Geyer, G. L. Klimchitskaya and V. M. Mostepanenko, *Phys. Rev.* **A67**, 062102 (2003).
26. S. G. Rabinovich, *Measurement Errors and Uncertainties. Theory and Practice* (Springer-Verlag, New York, 2000).
27. V. N. Granovskii and T. N. Siraya, *Methods for Experimental Data Processing in Measurements* (Energoatomizdat, Leningrad, 1990) (in Russian).
28. K. A. Brownlee, *Statistical Theory and Methodology in Science and Engineering* (Wiley, New York, 1965).
29. L. D. Landau, E. M. Lifshitz and L. P. Pitaevskii, *Electrodynamics of Continuous*

- Media* (Pergamon Press, Oxford, 1984).
30. *Handbook of Optical Constants of Solids*, ed. E. D. Palik (Academic, New York, 1985).
  31. G. L. Klimchitskaya, U. Mohideen and V. M. Mostepanenko, *Phys. Rev.* **A61**, 062107 (2000).
  32. I. Brevik, J. B. Aarseth, J. S. Høye and K. A. Milton, in *Quantum Field Theory Under the Influence of External Conditions*, ed. K. A. Milton (Rinton Press, Princeton 2004).
  33. K. A. Milton, *J. Phys.* **A37**, R209 (2004).
  34. B. Geyer, G. L. Klimchitskaya and V. M. Mostepanenko, *Phys. Rev.* **A70**, 016102 (2004).
  35. J. Heinrichs, *Phys. Rev.* **B11**, 3625 (1975); **B11**, 3637 (1975); **B12**, 6006 (1975).
  36. T. Emig, A. Hanke, R. Golestanian and M. Kardar, *Phys. Rev. Lett.* **87**, 260402 (2001); *Phys. Rev.* **A67**, 022114 (2003).
  37. P. Johansson and P. Apell, *Phys. Rev.* **B56**, 4159 (1997).
  38. M. Schaden and L. Spruch, *Phys. Rev.* **A58**, 935 (1998).
  39. A. Scardicchio and R. L. Jaffe, quant-ph/0406041.
  40. D. Iannuzzi, I. Gelfand, M. Lisanti and F. Capasso, in: *Quantum Field Theory Under the Influence of External Conditions*, ed. K. A. Milton (Rinton Press, Princeton, 2004).
  41. N. Arkani-Hamed, S. Dimopoulos and G. Dvali, *Phys. Rev.* **D59**, 086004 (1999).
  42. E. Fischbach and C. L. Talmadge, *The Search for Non-Newtonian Gravity* (Springer-Verlag, New York, 1999).
  43. Y. Su, B. R. Heckel, E. G. Adelberger, J. H. Gundlach, M. Harris, G. L. Smith and H. E. Swanson, *Phys. Rev.* **D50**, 3614 (1994).
  44. G. L. Smith, C. D. Hoyle, J. H. Gundlach, E. G. Adelberger, B. R. Heckel and H. E. Swanson, *Phys. Rev.* **D61**, 022001 (2000).
  45. J. K. Hoskins, R. D. Newman, R. Spero and J. Schultz, *Phys. Rev.* **D32**, 3084 (1985).
  46. C. D. Hoyle, U. Schmidt, B. R. Heckel, E. G. Adelberger, J. H. Gundlach, D. J. Kapner and H. E. Swanson, *Phys. Rev. Lett.* **86**, 1418 (2001).
  47. J. C. Long, H. W. Chan, A. B. Churnside, E. A. Gulbis, M. C. M. Varney and J. C. Price, *Nature* **421**, 922 (2003).
  48. J. Chiaverini, S. J. Smullin, A. A. Geraci, D. M. Weld and A. Kapitulnik, *Phys. Rev. Lett.* **90**, 151101 (2003).
  49. M. Bordag, B. Geyer, G. L. Klimchitskaya and V. M. Mostepanenko, *Phys. Rev.* **D58**, 075003 (1998).
  50. V. M. Mostepanenko, *Int. J. Mod. Phys.* **A17**, 722 (2002); **A17**, 4307 (2002).
  51. E. Fischbach, D. E. Krause, V. M. Mostepanenko and M. Novello, *Phys. Rev.* **D64**, 075010 (2001).
  52. F. Chen, G. L. Klimchitskaya, U. Mohideen and V. M. Mostepanenko, *Phys. Rev. Lett.* **90**, 160404 (2003).
  53. S. K. Lamoreaux and W. T. Buttler, quant-ph/0408027.